

# InGaAs 阱簇复合结构中镉原子自适应迁移的临界厚度

于庆南<sup>1\*</sup>, 刘子键<sup>1</sup>, 王新宇<sup>1</sup>, 李可<sup>1</sup>, 王茹<sup>1</sup>, 刘新雨<sup>1</sup>, 潘玉<sup>1</sup>, 李晖<sup>1</sup>, 张建伟<sup>2</sup>

<sup>1</sup>无锡学院江苏省集成电路可靠性技术及检测系统工程研究中心, 江苏 无锡 214105;

<sup>2</sup>中国科学院长春光学精密机械与物理研究所, 吉林 长春 130033

**摘要** 为了探究镉原子发生自适应迁移的临界厚度, 首先测量得到 InGaAs 阱簇复合结构表面不同位置的自发辐射光谱。镉原子的自适应迁移会导致阱簇复合结构中同时产生镉含量正常的和损失的  $\text{In}_x\text{Ga}_{1-x}\text{As}$  区域, 进而导致其自发辐射光谱具有特殊的双峰特征。通过对比光谱的双峰强度, 计算并评估了正常  $\text{In}_{0.17}\text{Ga}_{0.83}\text{As}$  层的厚度起伏为 4.6~6.4 nm, 即镉原子发生自适应迁移的临界厚度为 4.6 nm。通过对比 4 nm 传统 InGaAs 量子阱的单峰光谱特征, 验证了镉原子发生自适应迁移临界厚度的准确性, 该项研究对推动 InGaAs 阱簇复合量子限制结构的发展具有重要意义。

**关键词** 激光器; InGaAs/GaAs; 富镉团簇; 双峰光谱; 临界厚度

中图分类号 O432 文献标志码 A

DOI: 10.3788/AOS23090

## 1 引言

传统的高应变 InGaAs/GaAs 量子阱具有优良的特性, 已经被广泛应用于半导体激光器、红外探测器、电光调制器、太阳能电池等光电子器件<sup>[1-2]</sup>。近期本课题组基于富镉团簇(IRC)效应发现并提出一种特殊的 InGaAs 非对称阱簇复合(WCC)量子限制结构, 与传统 InGaAs/GaAs 量子阱统一的镉含量以及应变类型特点不同, 该结构可以在单一的 InGaAs 层中产生多种镉含量的有源区域, 同时具备离散的混合应变特征。这种特殊的 WCC 量子限制结构具有极其特殊的增益特性<sup>[3]</sup>, 对实现超宽调谐激光器和同步双频激光器具有重要研究意义<sup>[4-5]</sup>。由于 IRC 效应的形成会对传统量子限制器件的光学性能造成较大影响, 因此过去通常把 IRC 效应当成一种生长缺陷来规避, 忽略了其特殊的光学性能<sup>[6-7]</sup>。IRC 形成的基本原理是在生长高应变  $\text{In}_x\text{Ga}_{1-x}\text{As}/\text{GaAs}$  量子阱结构时,  $\text{In}_x\text{Ga}_{1-x}\text{As}$  材料内部的应力会随着材料生长厚度的增加逐渐积累, 为缓解高应变效应, 镉原子会自发地沿生长方向向顶部迁移, 在  $\text{In}_x\text{Ga}_{1-x}\text{As}$  材料表面堆积形成 IRC<sup>[8-9]</sup>。同时, 镉原子的迁移会使 InGaAs 上表面层区的镉含量降低, 在 InGaAs 有源区产生缺镉区域。由于镉原子的迁移是在应力积累到一定程度产生的, 即在生长高应变

$\text{In}_x\text{Ga}_{1-x}\text{As}/\text{GaAs}$  材料体系时会存在临界厚度  $h_c$ , 一旦超过该临界值, 应变将产生弛豫, 导致 IRC 效应形成。因此, 有效确定镉原子迁移的临界厚度, 对研究非对称 WCC 量子限制结构具有重要意义。

目前, 对于 WCC 结构中镉原子发生自适应迁移的临界厚度的研究较少, 而利用传统的量子阱厚度检测方法<sup>[10-13]</sup>(原子探针层析成像技术、X 射线双晶衍射技术和理论模拟技术)难以获得材料内部不同位置的厚度起伏情况, 进而无法准确评估  $\text{In}_x\text{Ga}_{1-x}\text{As}$  非对称 WCC 量子限制结构中镉原子的临界迁移厚度。因此, 本文通过收集 WCC 结构不同位置辐射的自发辐射(SE)光谱, 来研究  $\text{In}_x\text{Ga}_{1-x}\text{As}$  非对称 WCC 量子限制结构中正常  $\text{In}_{0.17}\text{Ga}_{0.83}\text{As}$  材料的厚度分布, 进而得到高应变导致镉原子迁移的临界厚度。

本文首先生长出  $\text{In}_x\text{Ga}_{1-x}\text{As}$  非对称 WCC 量子限制结构, 使用聚焦镜头将泵浦光聚焦为直径  $d=0.2$  mm 的光斑, 通过激励 WCC 结构的不同有源区域, 采集 WCC 芯片底部不同位置辐射的 SE 光谱。然后, 通过分析对比 SE 光谱的双峰强度, 利用 WCC 结构中正常  $\text{In}_{0.17}\text{Ga}_{0.83}\text{As}$  材料的厚度分布情况, 最终获得高应变镉基 WCC 量子限制结构中镉原子迁移的临界厚度。

收稿日期: 2023-05-04; 修回日期: 2023-05-24; 录用日期: 2023-05-31; 网络首发日期: 2023-06-28

基金项目: 国家自然科学基金(62204172)、江苏省高等学校基础科学(自然科学)研究项目(22KJB140016)、江苏省双创博士项目(JSSCBS20210870, JSSCBS20210868)、南京信息工程大学滨江学院人才启动经费(550221009, 550221036)

通信作者: \*yuqingnan1@126.com

## 2 非对称 WCC 结构及双峰 SE 光谱

首先在 GaAs 衬底上生长出 InGaAs 非对称 WCC 量子限制结构。为了在有源区中引入足够的应力及应变积累,所采用的 InGaAs 层厚为 10 nm,具体材料为  $\text{In}_{0.17}\text{Ga}_{0.83}\text{As}$ 。InGaAs 有源层两侧为 2 nm 厚的 GaAs 应变补偿层,以促进 IRC 的形成并控制 InGaAs 和势垒层之间的应变。补偿层外侧为 8 nm 厚的  $\text{GaAs}_{0.92}\text{P}_{0.08}$  势垒层,用于吸收泵浦光,该 InGaAs 非对称 WCC 量子限制结构如图 1 所示。只有当 InGaAs 层厚超过临界厚度  $h_c$  时,镉原子才会 在高应力作用下产生自适应迁移。为了方便进行实验操作,该 WCC 结构的长和

宽分别被设计为 3.0 mm 和 1.5 mm。为了获得明显的 IRC 效应,产生较强的镉原子迁移,InGaAs 层的厚度不能低于临界厚度<sup>[14]</sup>,且 In 含量不宜过低<sup>[15]</sup>。WCC 样品在 660 °C 和  $10^4$  Pa 的压力下以  $0.7 \mu\text{m}/\text{h}$  的速率沉积。采用较高的生长温度是为了增加镉原子的迁移长度,有利于材料生长中 IRC 效应的形成<sup>[16]</sup>。为确保生长的 WCC 结构中包含 IRC 效应,使用原子力显微镜 (Park Systems Instrument Co., Ltd., 型号 XE100) 测量 InGaAs 上表面的形貌特征,结果如图 1 插图所示。该显微图像展现出大量不规则的三维团簇形貌,说明该结构发生了较强的镉原子迁移,形成了明显的 IRC 效应。

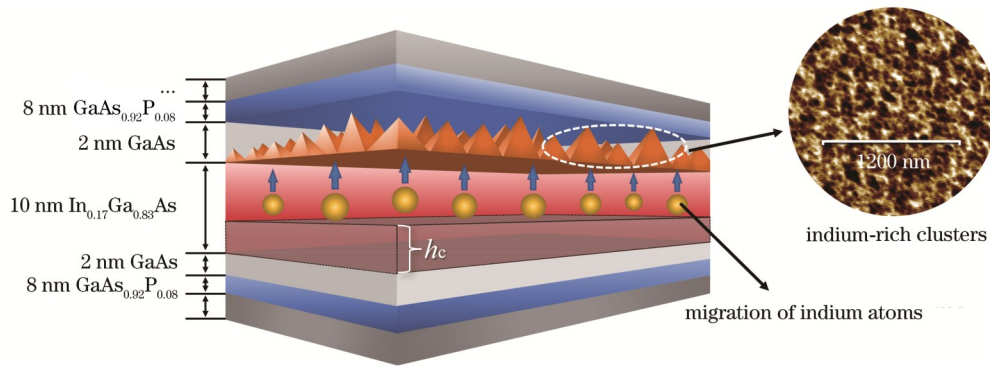


图 1 InGaAs/GaAs 非对称 WCC 量子限制结构及 IRC 的形貌特征

Fig. 1 InGaAs/GaAs asymmetric WCC quantum-confined structure and appearance characteristics of IRC

InGaAs/GaAs 材料体系存在较严重的晶格失配,在生长过程中会引入较大的应变积累,进而导致镉原子通过自适应迁移来释放应力。同时镉原子的迁移又会降低相应  $\text{In}_{0.17}\text{Ga}_{0.83}\text{As}$  区域的镉含量,产生非对称 WCC 量子限制结构。根据本课题组的前期研究,该非对称 WCC 结构有源区中主要包含镉含量正常的  $\text{In}_{0.17}\text{Ga}_{0.83}\text{As}$  层和镉含量损失的  $\text{In}_{0.12}\text{Ga}_{0.88}\text{As}$  层<sup>[7]</sup>。为了探究镉原子发生自适应迁移的临界厚度  $h_c$ ,搭建了

图 2 右侧插图所示的实验测量系统。使用 808 nm 激光器作为泵浦光源,通过聚焦镜头使光束会聚为直径  $d=0.2 \text{ mm}$  的圆形泵浦光斑,确保泵浦光以固定面积注入样品的待测区域。从泵浦区域对应的样品底部测量 WCC 结构辐射的 SE 光谱,通过改变泵浦光注入的位置,逐点测量整个 WCC 样品中各位置的 SE 光谱。其中 A、B、C 3 个不同有源区辐射的 SE 光谱如图 2 所示。

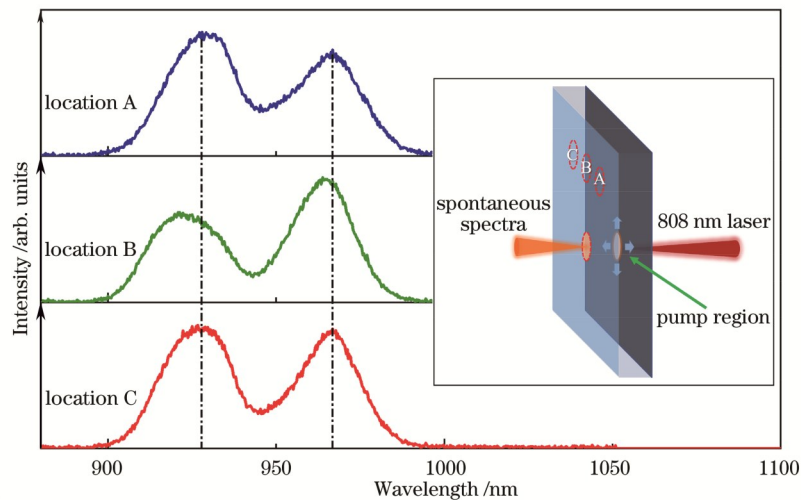


图 2 WCC 结构的双峰 SE 光谱及实验测量系统

Fig. 2 SE spectra with dual peaks emitted from WCC structure and experimental measurement system

### 3 结果与分析

图 2 显示了  $\text{In}_x\text{Ga}_{1-x}\text{As}$  非对称 WCC 样品在注入载流子浓度为  $N=4.8 \times 10^{17} \text{ cm}^{-3}$  时 3 个不同位置辐射的 SE 光谱。与传统量子阱产生的单峰辐射 SE 光谱不同, WCC 结构不同位置辐射的 SE 光谱都呈现出明显的双峰特征, 且双峰强度存在不同程度的起伏变化。出现该双峰特征的原因主要是镉原子自适应迁移, 导致有源区同时存在镉含量正常的  $\text{In}_{0.17}\text{Ga}_{0.83}\text{As}$  层和镉含量损失的  $\text{In}_{0.12}\text{Ga}_{0.88}\text{As}$  层, 以上两种  $\text{In}_x\text{Ga}_{1-x}\text{As}$  材料具有不同的禁带宽度, 且所辐射的光子能量不同, 进而产生了这种特殊的双峰光谱。双峰强度的起伏变化则说明以上两种材料具有不同的有源层厚度。因此, 可以通过分析 SE 光谱的双峰强度来确定二者的厚度分布, 进而得到镉原子进行初始迁移时的临界厚度  $h_c$ 。

SE 光谱强度与  $\text{In}_x\text{Ga}_{1-x}\text{As}$  激活层厚度之间的关系<sup>[17]</sup>可表示为

$$P = (\gamma BN^2 hcsL) / [n\lambda(1 - R_1 R_2)^2], \quad (1)$$

式中:  $P$  为 SE 光谱的强度;  $L$  为有源层厚度;  $\gamma$  为量子效率;  $B$  为双分子复合系数;  $N$  为载流子浓度;  $h$  为普朗克常数;  $c$  为光速;  $s$  为 IRC 器件面积;  $n$  为折射率;  $\lambda$  为辐射波长;  $R_1$  和  $R_2$  为两个端面的反射率。

根据式(1), SE 光谱的强度  $P$  与有源层厚度  $L$  以及辐射波长  $\lambda$  的关系为  $P \propto L/\lambda$ 。室温下  $\text{In}_x\text{Ga}_{1-x}\text{As}$  材料的禁带宽度  $E_g$  和  $x$  之间的关系<sup>[18]</sup>为

$$E_g = 1.42 - 1.49x + 0.43x^2. \quad (2)$$

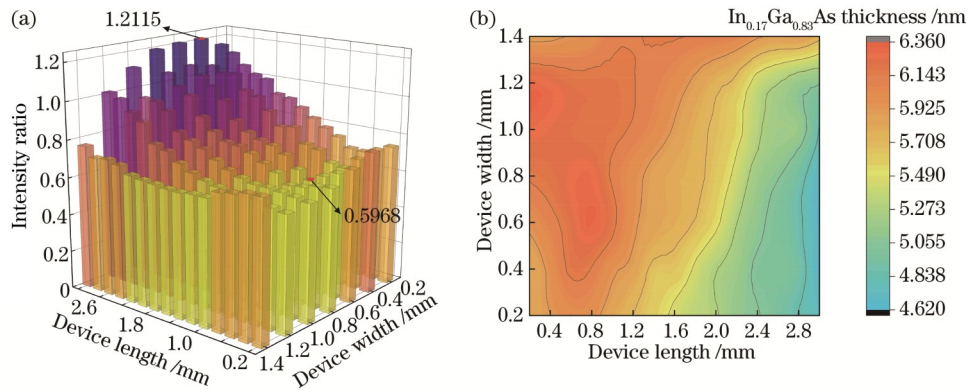


图 3 材料厚度分布情况。(a)  $\text{In}_{0.17}\text{Ga}_{0.83}\text{As}$  和  $\text{In}_{0.12}\text{Ga}_{0.88}\text{As}$  自发辐射强度比值; (b)  $\text{In}_{0.17}\text{Ga}_{0.83}\text{As}$  层厚度的等高线图

Fig. 3 Material thickness distribution. (a) Ratio of spontaneous emission intensity of  $\text{In}_{0.17}\text{Ga}_{0.83}\text{As}$  and  $\text{In}_{0.12}\text{Ga}_{0.88}\text{As}$ ; (b) contour of  $\text{In}_{0.17}\text{Ga}_{0.83}\text{As}$  layer thickness

为了说明以上结论的准确性, 在相同的载流子浓度 ( $N=4.8 \times 10^{17} \text{ cm}^{-3}$ ) 下测量得到有源层厚度为 4 nm 的  $\text{InGaAs}$  量子阱的 SE 光谱, 该光谱呈现出典型的单峰形状, 光谱曲线与 WCC 结构 SE 光谱的对比结果如图 4 所示。这一结果表明, 在 4 nm 厚的  $\text{In}_{0.17}\text{Ga}_{0.83}\text{As}/\text{GaAs}$  材料中并未发生镉原子迁移, 即 IRC 效应。这主要是因为 4 nm 的  $\text{In}_{0.17}\text{Ga}_{0.83}\text{As}$  材料厚度尚未达到镉原子迁移的临界厚度  $h_c$ , 材料中积累的

由式(2)可知,  $\text{In}_{0.17}\text{Ga}_{0.83}\text{As}$  层的带隙小于  $\text{In}_{0.12}\text{Ga}_{0.88}\text{As}$  层的禁带宽度, 因此图 2 所示双峰 SE 光谱中的右侧谱峰主要由  $\text{In}_{0.17}\text{Ga}_{0.83}\text{As}$  层产生, 对应的中心波长  $\lambda_{0.17}=966 \text{ nm}$ , 左侧谱峰主要由  $\text{In}_{0.12}\text{Ga}_{0.88}\text{As}$  材料产生, 对应的中心波长  $\lambda_{0.12}=927 \text{ nm}$ 。

基于以上分析, 通过图 2 测量的 WCC 结构不同位置辐射的双峰 SE 光谱, 计算获得 SE 光谱中双峰的强度比值, 计算结果如图 3(a) 所示。图中展示了 WCC 材料各位置中  $\text{In}_{0.17}\text{Ga}_{0.83}\text{As}$  与  $\text{In}_{0.12}\text{Ga}_{0.88}\text{As}$  的 SE 光谱双峰比值(右峰与左峰的强度之比), 其中强度比的最大值为 1.2115, 最小值为 0.5968。通过式(1)计算得到  $\text{In}_{0.17}\text{Ga}_{0.83}\text{As}$  层对应的厚度分别为 4.6 nm 和 6.4 nm。为了更直观地呈现出 WCC 结构中正常  $\text{In}_{0.17}\text{Ga}_{0.83}\text{As}$  材料的厚度起伏, 绘制出其厚度等高线, 如图 3(b) 所示。可以看到,  $\text{In}_{0.17}\text{Ga}_{0.83}\text{As}$  层的厚度分布为 4.6~6.4 nm。不同位置  $\text{In}_{0.17}\text{Ga}_{0.83}\text{As}$  层的厚度不同, 这主要是因为镉原子的迁移会导致不均匀的应变积累以及分布, 从而导致不同位置产生的 IRC 效应有所不同, 并形成图 1 中大小不一的 IRC。由于镉原子的自适应迁移是在  $\text{In}_{0.17}\text{Ga}_{0.83}\text{As}$  层厚度达到临界厚度  $h_c$  后产生的, 因此临界厚度  $h_c$  以下为正常的  $\text{In}_{0.17}\text{Ga}_{0.83}\text{As}$  材料。这意味着只要  $\text{In}_{0.17}\text{Ga}_{0.83}\text{As}$  层的生长厚度不超过 4.6 nm, 镉原子就不会发生自适应迁移。这是因为此时材料的应变积累较小, 不足以产生 IRC 效应。综上所述, 镉原子发生自适应迁移的临界厚度可以被评估为 4.6 nm。

应变不足以导致 IRC 效应的产生。此外, 文献[19]的研究结果表明, 对于  $\text{In}_{0.15}\text{Ga}_{0.85}\text{As}/\text{GaAs}$  材料结构, 当层厚大于 6 nm 时, 会出现明显的双峰现象, 这说明镉原子发生了迁移, 引发了 IRC 效应。本文采用的  $\text{In}_{0.17}\text{Ga}_{0.83}\text{As}/\text{GaAs}$  材料的晶格失配率为 1.2%, 相对  $\text{In}_{0.15}\text{Ga}_{0.85}\text{As}/\text{GaAs}$  材料(失配率为 1.1%)具有更严重的晶格失配, 更容易产生较大的应变积累, 从而更容易产生镉原子迁移, 以上结果也进一步验证了本文测量

结果的准确性。以上分析结果与实验结论一致,验证了 WCC 结构中发生铜原子迁移的临界厚度的准确性。该方法不仅可以获得非对称 WCC 量子限制结构中不同铜含量  $\text{In}_x\text{Ga}_{1-x}\text{As}$  材料的厚度分布,还可以确定高应变量子阱中发生铜原子迁移的临界厚度,对  $\text{In}_x\text{Ga}_{1-x}\text{As}$  非对称 WCC 结构的研究和发展具有重要意义。

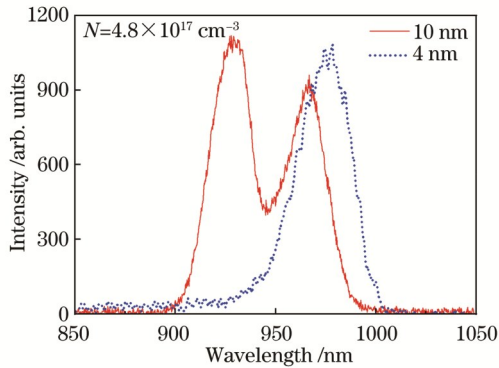


图 4 WCC 样品和 4 nm  $\text{In}_{0.17}\text{Ga}_{0.83}\text{As}$  量子阱的 SE 光谱  
Fig. 4 SE spectra of WCC sample and 4 nm thick  $\text{In}_{0.17}\text{Ga}_{0.83}\text{As}$  quantum well

## 4 结 论

通过逐个测量材料表面不同位置辐射的自发辐射光谱,计算得到  $\text{InGaAs}$  非对称 WCC 量子限制结构中铜原子迁移的临界厚度。通过将泵浦光束聚焦到 WCC 样品的局部表面来逐次测量不同泵浦区域辐射的 SE 光谱。通过分析 SE 光谱的双峰强度及比值,获得铜含量正常的  $\text{In}_{0.17}\text{Ga}_{0.83}\text{As}$  层厚度波动为 4.6~6.4 nm,进而确定了铜原子迁移的临界厚度为 4.6 nm。该研究内容对于  $\text{In}_x\text{Ga}_{1-x}\text{As}$  非对称 WCC 量子限制结构的发展和应用具有重要价值。

## 参 考 文 献

- [1] 唐恒敬, 吕衍秋, 张可锋, 等. 空间遥感器  $\text{InGaAs}$  短波红外探测器[J]. 激光与光电子学进展, 2007, 44(5): 42-49.  
Tang H J, Lü Y Q, Zhang K F, et al. Short-wavelength infrared  $\text{InGaAs}$  photodetector for spatial remote sensing[J]. Laser & Optoelectronics Progress, 2007, 44(5): 42-49.
- [2] 黄润宇, 赵伟林, 曾辉, 等.  $\text{InP}$  基单光子探测器的发展和应用[J]. 激光与光电子学进展, 2021, 58(10): 1011009.  
Huang R Y, Zhao W L, Zeng H, et al. Development and application of  $\text{InP}$ -based single photon detectors[J]. Laser & Optoelectronics Progress, 2021, 58(10): 1011009.
- [3] Yu Q N, Meng Y H, Li K, et al. Luminescence mechanism of  $\text{InGaAs}$  self-fit well-cluster composite structure with super-wide spectra[J]. Journal of Luminescence, 2023, 253: 119435.
- [4] Yu Q N, Li X, Jia Y, et al.  $\text{InGaAs}$ -based well-island composite quantum-confined structure with superwide and

- uniform gain distribution for great enhancement of semiconductor laser performance[J]. ACS Photonics, 2018, 5(12): 4896-4902.
- [5] Yu Q N, Zheng M, Tai H X, et al. Quantum confined indium-rich cluster lasers with polarized dual-wavelength output[J]. ACS Photonics, 2019, 6(8): 1990-1995.
- [6] 林楠, 仲莉, 黎海明, 等. 应变补偿多量子阱结构半导体可饱和吸收镜[J]. 中国激光, 2022, 49(11): 1101002.  
Lin N, Zhong L, Li H M, et al. Strain-compensated multi-quantum well structure semiconductor saturable absorption mirror[J]. Chinese Journal of Lasers, 2022, 49(11): 1101002.
- [7] Kryzhanovskaya N V, Moiseev E I, Zubov F I, et al. Direct modulation characteristics of microdisk lasers with  $\text{InGaAs}/\text{GaAs}$  quantum well-dots[J]. Photonics Research, 2019, 7(6): 664-668.
- [8] Yu H P, Roberts C, Murray R. Influence of indium segregation on the emission from  $\text{InGaAs}/\text{GaAs}$  quantum wells[J]. Applied Physics Letters, 1995, 66(17): 2253-2255.
- [9] Schlenker D, Miyamoto T, Chen Z, et al. Growth of highly strained  $\text{GaInAs}/\text{GaAs}$  quantum wells for 1.2  $\mu\text{m}$  wavelength lasers[J]. Journal of Crystal Growth, 2000, 209(1): 27-36.
- [10] Bennett S E, Saxey D W, Kappers M J, et al. Atom probe tomography assessment of the impact of electron beam exposure on  $\text{In}_x\text{Ga}_{1-x}\text{N}/\text{GaN}$  quantum wells[J]. Applied Physics Letters, 2011, 99(2): 021906.
- [11] Yuan K, Radhakrishnan K, Zheng H Q, et al. Characterization of linearly graded metamorphic  $\text{InGaP}$  buffer layers on  $\text{GaAs}$  using high-resolution X-ray diffraction[J]. Thin Solid Films, 2001, 391(1): 36-41.
- [12] Ferrari C, Bruni M R, Martelli F, et al.  $\text{InGaAs}/\text{GaAs}$  strained single quantum well characterization by high resolution X-ray diffraction[J]. Journal of Crystal Growth, 1993, 126(1): 144-150.
- [13] Yang T J, Shivaraman R, Speck J S, et al. The influence of random indium alloy fluctuations in indium gallium nitride quantum wells on the device behavior[J]. Journal of Applied Physics, 2014, 116(11): 113104.
- [14] 刘洋, 李林, 乔忠良, 等. MOCVD 生长 1.06  $\mu\text{m}$  波段  $\text{InGaAs}/\text{GaAs}$  单量子阱材料的发光特性研究[J]. 中国激光, 2014, 41(11): 1106001.  
Liu Y, Li L, Qiao Z L, et al. Optical characteristics of 1.06  $\mu\text{m}$   $\text{InGaAs}/\text{GaAs}$  quantum well grown by MOCVD[J]. Chinese Journal of Lasers, 2014, 41(11): 1106001.
- [15] 徐华伟, 宁永强, 曾玉刚, 等. 反射各向异性谱在线监测 852 nm 半导体激光器  $\text{AlGaInAs}/\text{AlGaAs}$  量子阱的 MOCVD 外延生长[J]. 中国激光, 2012, 39(5): 0502010.  
Xu H W, Ning Y Q, Zeng Y G, et al. MOCVD growth of  $\text{AlGaInAs}/\text{AlGaAs}$  quantum well for 852 nm laser diodes studied by reflectance anisotropy spectroscopy[J]. Chinese Journal of Lasers, 2012, 39(5): 0502010.
- [16] Jasik A, Wnuk A, Wójcik-Jedlińska A, et al. The influence of the growth temperature and interruption time on the crystal quality of  $\text{InGaAs}/\text{GaAs}$  QW structures grown by MBE and MOCVD methods[J]. Journal of Crystal Growth, 2008, 310(11): 2785-2792.
- [17] Basu P K, Mukhopadhyay B, Basu R. Semiconductor laser theory[M]. Boston: CRC Press, 2015.
- [18] Goldberg Y A, Schmidt N M. Handbook series on semiconductor parameters[M]. London: World Scientific, 1999: 62-88.
- [19] Yu H P, Roberts C, Murray R. Influence of indium segregation on the emission from  $\text{InGaAs}/\text{GaAs}$  quantum wells[J]. Applied Physics Letters, 1995, 66(17): 2253-2255.

# Critical Thickness of Indium Atom Self-Fitting Migration in InGaAs Well-Cluster Composite Structure

Yu Qingnan<sup>1\*</sup>, Liu Zijian<sup>1</sup>, Wang Xinyu<sup>1</sup>, Li Ke<sup>1</sup>, Wang Ru<sup>1</sup>, Liu Xinyu<sup>1</sup>, Pan Yu<sup>1</sup>, Li Hui<sup>1</sup>, Zhang Jianwei<sup>2</sup>

<sup>1</sup>Jiangsu Province Engineering Research Center of Integrated Circuit Reliability Technology and Testing System, Wuxi University, Wuxi 214105, Jiangsu, China;

<sup>2</sup>Changchun Institute of Optics, Fine Mechanics and Physics, Chinese Academy of Sciences, Changchun 130033, Jilin, China

## Abstract

**Objective** In recent years, a novel InGaAs well-cluster composite (WCC) quantum-confined structure has been demonstrated that the special structure has excellent optical properties, which are important for the realization of ultra-wide tunable lasers and synchronous dual-wavelength lasers. The WCC structure is based on the self-fit migration of indium atoms caused by the indium-rich cluster (IRC) effect, which are typically regarded as defects to be avoided for the conventional InGaAs quantum-well structure. Therefore, its special optical characteristics remain neglected. The formation mechanism of this WCC structure is based on the migration of indium atoms under high strain background. The strain will gradually accumulate with the continuous deposition of InGaAs material thickness. In order to relax the high strain in the InGaAs layer, indium atoms would automatically migrate along the material growth direction and form IRCs after the  $\text{In}_x\text{Ga}_{1-x}\text{As}$  is grown to exceed the critical thickness on the GaAs. Therefore, how to effectively determine the critical thickness of indium atom migration is of great significance for the study of WCC structures. However, there is little research on the critical thickness of the WCC structure. The traditional measurement methods on quantum well thickness make it difficult to obtain the thickness fluctuations at different positions. Furthermore, it is not possible to accurately evaluate the critical thickness of indium atom migration in the asymmetric  $\text{In}_x\text{Ga}_{1-x}\text{As}$  WCC structure. Therefore, the critical thickness of indium atom migration is investigated by collecting spontaneous emission (SE) spectra from different positions in the WCC structure.

**Methods** First, in order to study the critical thickness of indium atom self-fit migration in the IRC effect, an asymmetrical InGaAs WCC quantum confinement structure is grown on a GaAs substrate. Because IRCs generally occur in highly strained InGaAs/GaAs systems, the active layer used  $\text{In}_{0.17}\text{Ga}_{0.83}\text{As}/\text{GaAs}/\text{GaAs}_{0.92}\text{P}_{0.08}$ . The thickness of the  $\text{In}_{0.17}\text{Ga}_{0.83}\text{As}$  layer is designed to be 10 nm because an InGaAs layer thinner than 10 nm is insufficient to obtain the IRC effect. Second, in order to measure SE spectra, the sample is processed to obtain a 3.0 mm × 1.5 mm configuration. The device is vertically pumped from a fiber-coupled 808 nm pulsed laser at room temperature. The pump beam is focused into a 0.2 mm diameter spot. The fiber coupler is used to collect the SE spectra emitted from the corresponding pumping region from the bottom of the WCC structure. The SE spectra from different positions of the WCC structure are measured by moving the sample. The SE spectra exhibit typical bimodal characteristics. The formation mechanism is that the self-fit migration of the indium atoms in the WCC structure would reduce the indium content in the corresponding InGaAs regions, consequently generating normal and indium-deficient  $\text{In}_x\text{Ga}_{1-x}\text{As}$  regions. The spectra with dual peaks come from the superposition of spectra emitted from the normal  $\text{In}_{0.17}\text{Ga}_{0.83}\text{As}$  layer and indium-deficient  $\text{In}_{0.12}\text{Ga}_{0.88}\text{As}$  layer with different band gaps. The intensity fluctuation of the dual peaks mainly depends on the thickness fluctuation of the two materials. Third, the critical thickness can be evaluated by comparing the intensity of dual peaks.

**Results and Discussions** The self-fit migration of indium atoms leads to the formation of both normal  $\text{In}_{0.17}\text{Ga}_{0.83}\text{As}$  and indium-deficient  $\text{In}_{0.12}\text{Ga}_{0.88}\text{As}$  regions in the WCC structure. The bimodal configuration in the spontaneous emission spectra is a remarkable feature of the IRC effect taking place in the InGaAs-based WCC structure. The SE intensity mainly depends on the  $\text{In}_x\text{Ga}_{1-x}\text{As}$  material thickness  $L$  and the peak wavelength  $\lambda$ . Based on the dual peaks in SE spectra from different positions of the WCC structure, the intensity ratio of the dual peaks can be calculated, with a maximum intensity ratio of 1.2115 and a minimum value of 0.5968. The thickness of the  $\text{In}_{0.17}\text{Ga}_{0.83}\text{As}$  layer corresponds to 4.6 nm and 6.4 nm, respectively (Fig. 3). Due to the migration of indium atoms occurring after the thickness of the  $\text{In}_{0.17}\text{Ga}_{0.83}\text{As}$  layer reaches the critical thickness, the material within the critical thickness is normal  $\text{In}_{0.17}\text{Ga}_{0.83}\text{As}$  material. This means that as long as the growth thickness of the  $\text{In}_{0.17}\text{Ga}_{0.83}\text{As}$  layer does not exceed 4.6 nm, indium atoms will not migrate. This is because the strain accumulation is not sufficient to generate the IRC effect. In summary, the critical thickness for

self-fit migration of indium atoms can be evaluated as approximately 4.6 nm. Finally, in order to illustrate the accuracy of this conclusion, the spontaneous emission spectrum of a 4 nm thick  $\text{In}_{0.17}\text{Ga}_{0.83}\text{As}/\text{GaAs}$  compressively strained quantum well is collected under the same injected carrier density. It is found that there is only one peak in the spectra (Fig. 4). The result indicates that indium atoms do not migrate to form IRCs in the 4 nm thick  $\text{In}_{0.17}\text{Ga}_{0.83}\text{As}/\text{GaAs}$  material. Although there is strain accumulation in the 4 nm thick  $\text{In}_{0.17}\text{Ga}_{0.83}\text{As}$  material, it is not enough to produce the IRC effect. Therefore, the bimodal configuration in spectra disappears. This is consistent with the experimental results, which demonstrate the relative accuracy of the conclusion.

**Conclusions** In this paper, the critical thickness of indium atom migration in InGaAs asymmetric WCC quantum confinement structures is calculated by measuring the spontaneous emission spectra emitted from the different positions of the WCC structure. The SE spectra emitted from different pump regions are measured by focusing the pump beam on the local surface of the WCC sample. By analyzing the bimodal intensity and ratio of the SE spectra, the normal  $\text{In}_{0.17}\text{Ga}_{0.83}\text{As}$  layer thickness fluctuation of 4.6–6.4 nm is obtained. Furthermore, the critical thickness for the migration of indium atoms is determined to be approximately 4.6 nm. This research content has important value for the development and application of  $\text{In}_x\text{Ga}_{1-x}\text{As}$  asymmetric WCC quantum confinement structures.

**Key words** lasers; InGaAs/GaAs; indium-rich cluster; dual peak spectrum; critical thickness